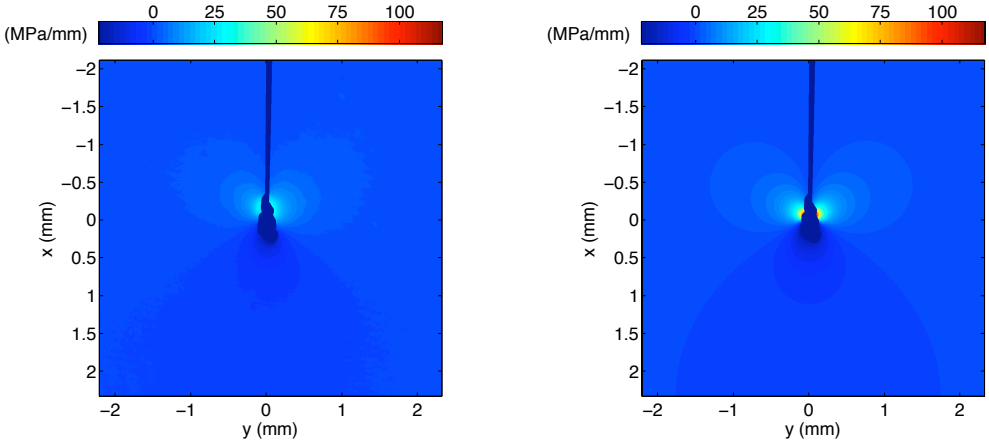

(a) Experimental $\frac{\partial(\sigma_1+\sigma_2)}{\partial x}$

(b) Theoretical $\frac{\partial(\sigma_1+\sigma_2)}{\partial x}$

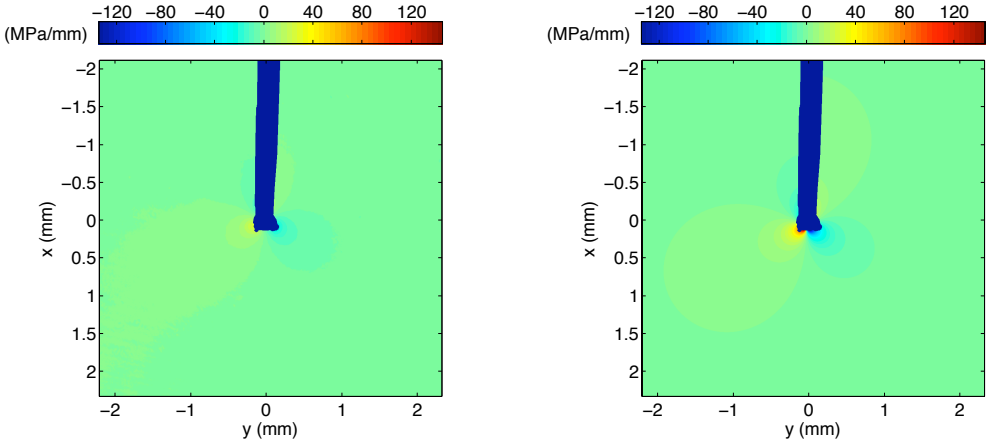

(c) Experimental $\frac{\partial(\sigma_1+\sigma_2)}{\partial y}$

(d) Theoretical $\frac{\partial(\sigma_1+\sigma_2)}{\partial y}$

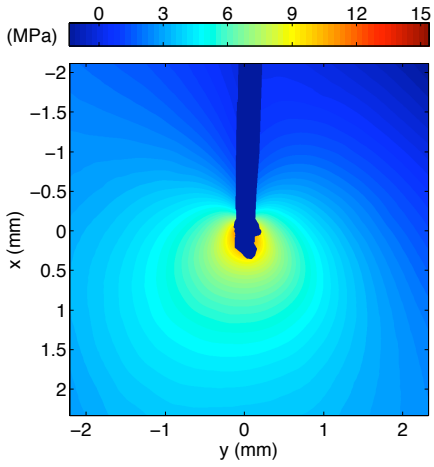

(e) Experimental $\sigma_1 + \sigma_2$

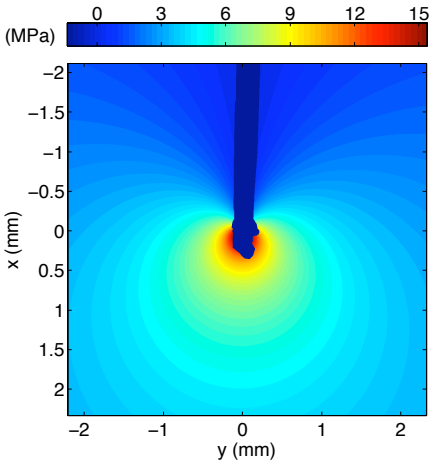

(f) Theoretical $\sigma_1 + \sigma_2$

Figure 4.40: Experimental and theoretical data for the derivatives of $\sigma_1 + \sigma_2$ and the experimental integrated $\sigma_1 + \sigma_2$ for specimen HomC1 for $K_I = 0.259$ MPa$\sqrt{\text{m}}$ and $K_{II} = 5.0$ kPa$\sqrt{\text{m}}$ with crack region masked in blue

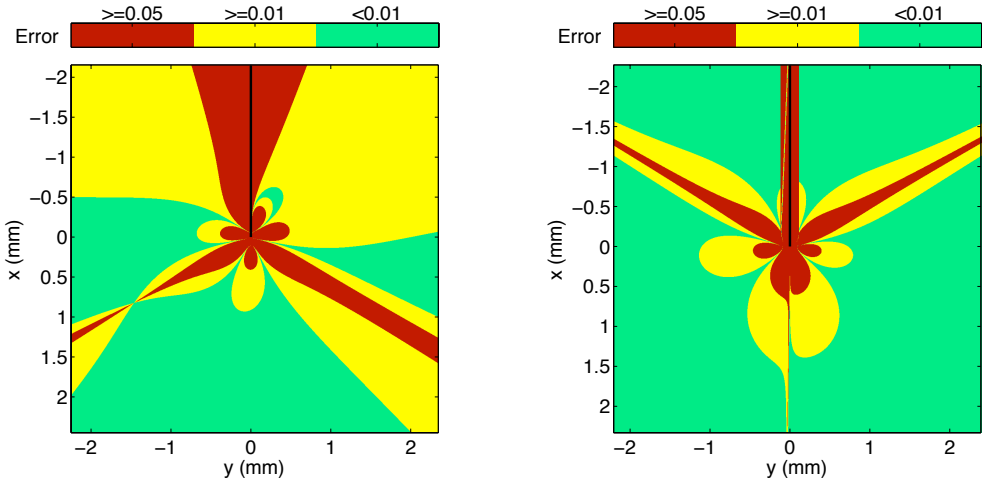

(a) Error for vertical shearing direction

(b) Error for horizontal shearing direction

Figure 4.41: Theoretical error for CGS approximating the derivatives of $\sigma_1+\sigma_2$, assuming $K_I = 0.259$ MPa$\sqrt{\text{m}}$ and $K_{II} = 5.0$ kPa$\sqrt{\text{m}}$ for the 4.6 mm $\times$ 4.6 mm field of view and lateral shearing distance of $d_{shear} = 225$ μm [Crack indicated in black]

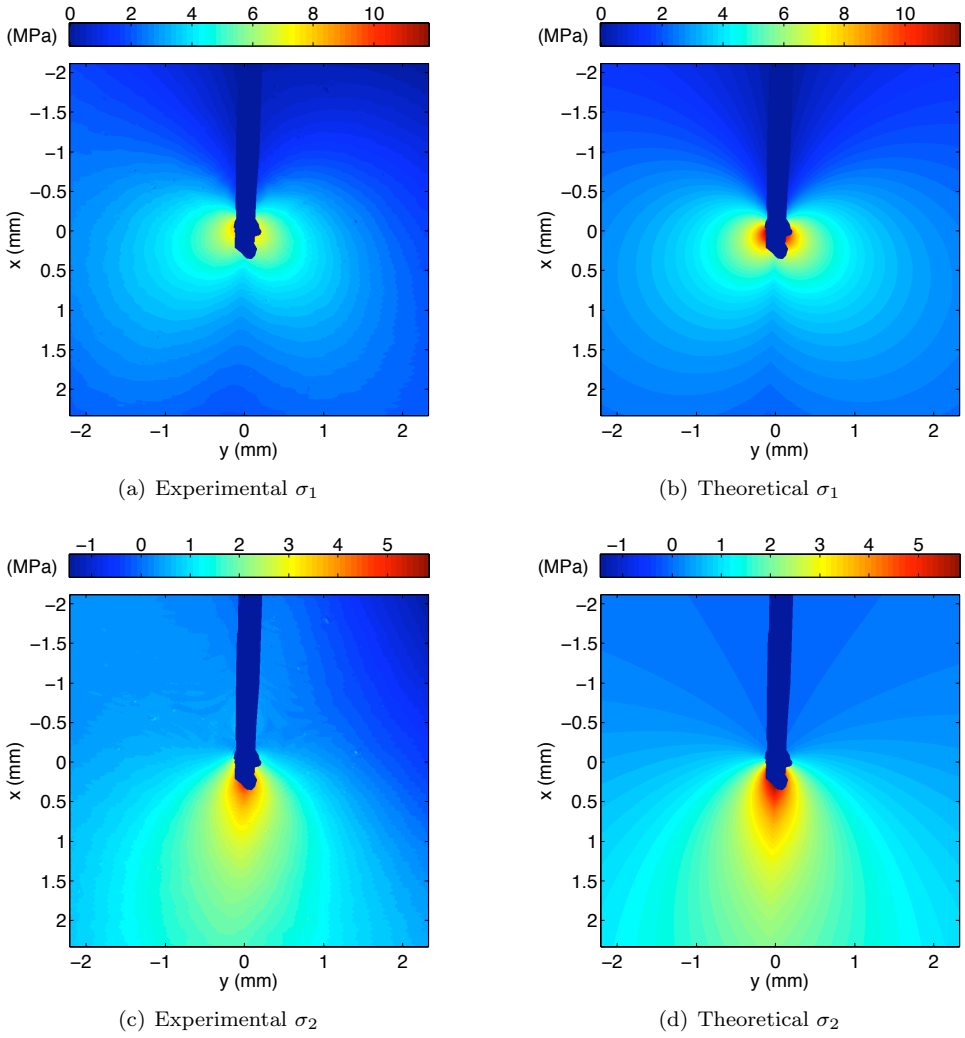

(a) Experimental σ_1

(b) Theoretical σ_1

(c) Experimental σ_2

(d) Theoretical σ_2

Figure 4.42: Experimental and theoretical data for the principal stresses for specimen HomC1 for $K_I = 0.259$ MPa$\sqrt{\text{m}}$ and $K_{II} = 5.0$ kPa$\sqrt{\text{m}}$ with crack region masked in blue

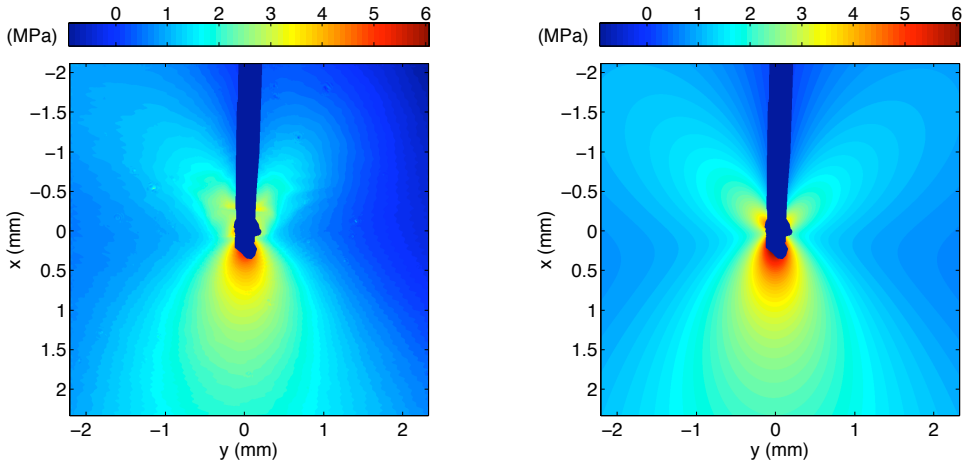

(a) Experimental σ_{xx}

(b) Theoretical σ_{xx}

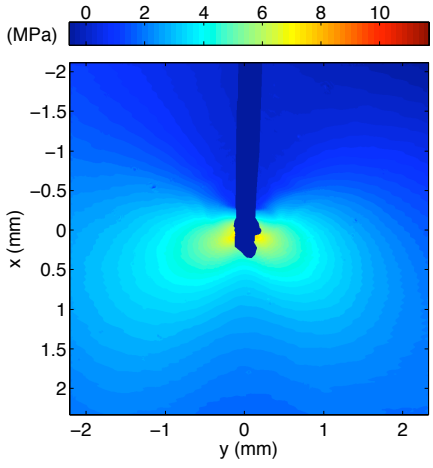

(c) Experimental σ_{yy}

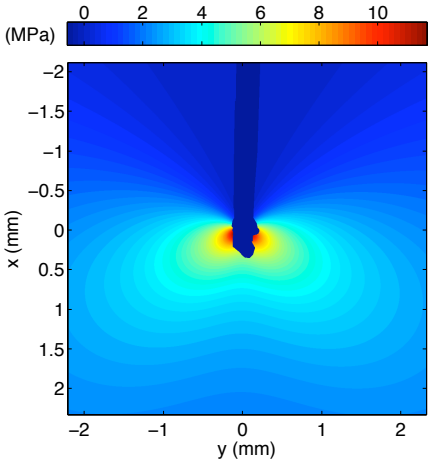

(d) Theoretical σ_{yy}

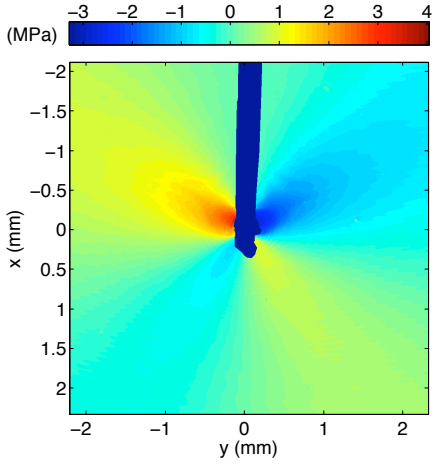

(e) Experimental σ_{xy}

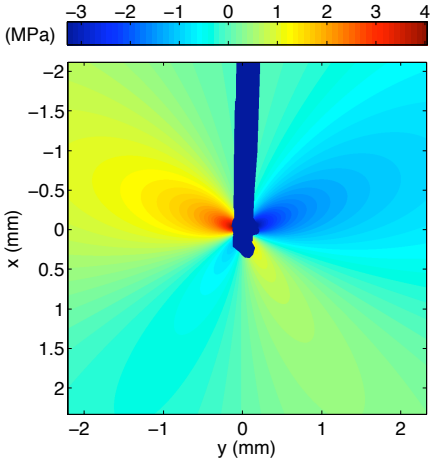

(f) Theoretical σ_{xy}

Figure 4.43: Experimental and theoretical data for the Cartesian stresses for specimen HomC1 for $K_I = 0.259$ MPa$\sqrt{\text{m}}$ and $K_{II} = 5.0$ kPa$\sqrt{\text{m}}$ with crack region masked in blue

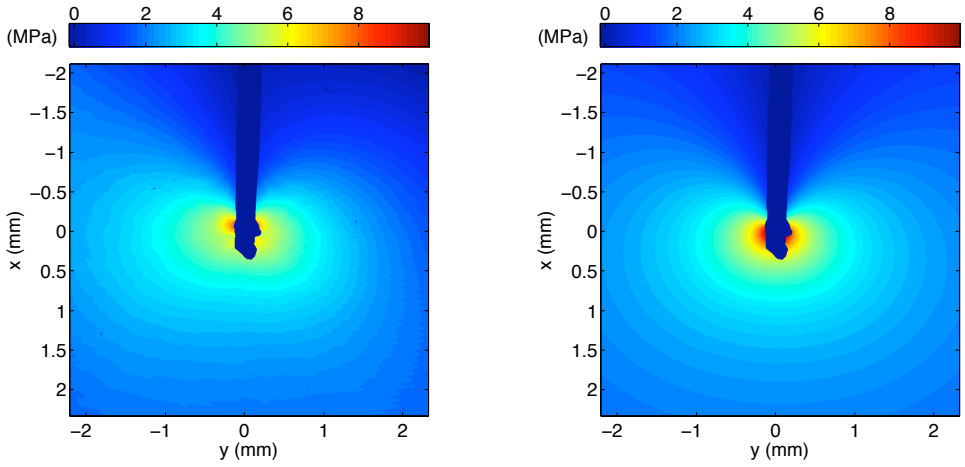

(a) Experimental σ_{rr}

(b) Theoretical σ_{rr}

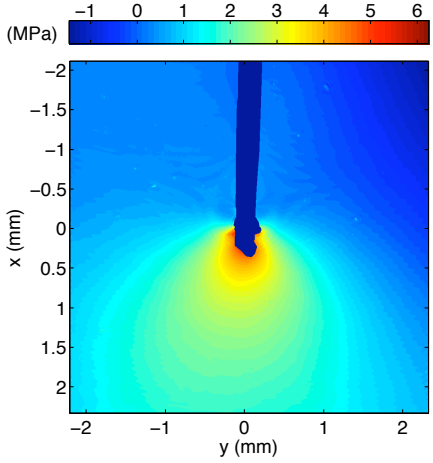

(c) Experimental $\sigma_{\theta\theta}$

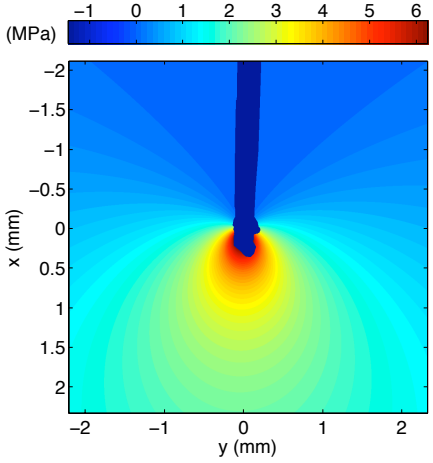

(d) Theoretical $\sigma_{\theta\theta}$

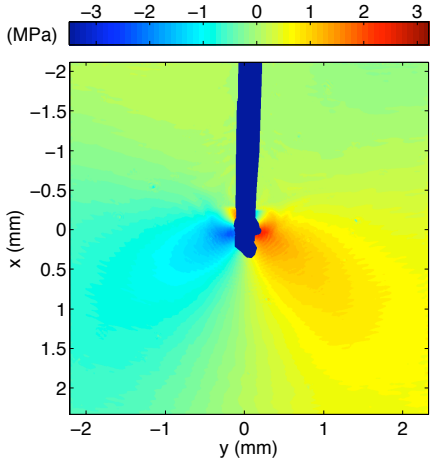

(e) Experimental $\sigma_{r\theta}$

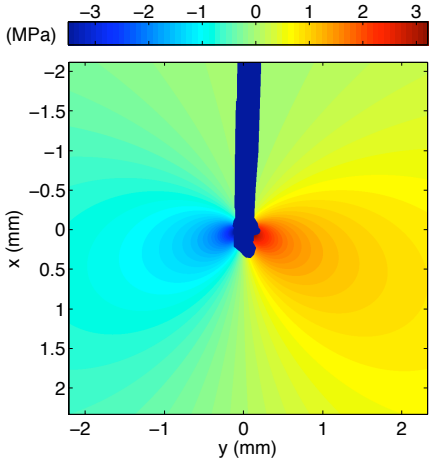

(f) Theoretical $\sigma_{r\theta}$

Figure 4.44: Experimental and theoretical data for the polar stresses for specimen HomC1 for $K_I = 0.259$ MPa$\sqrt{\text{m}}$ and $K_{II} = 5.0$ kPa$\sqrt{\text{m}}$ with crack region masked in blue

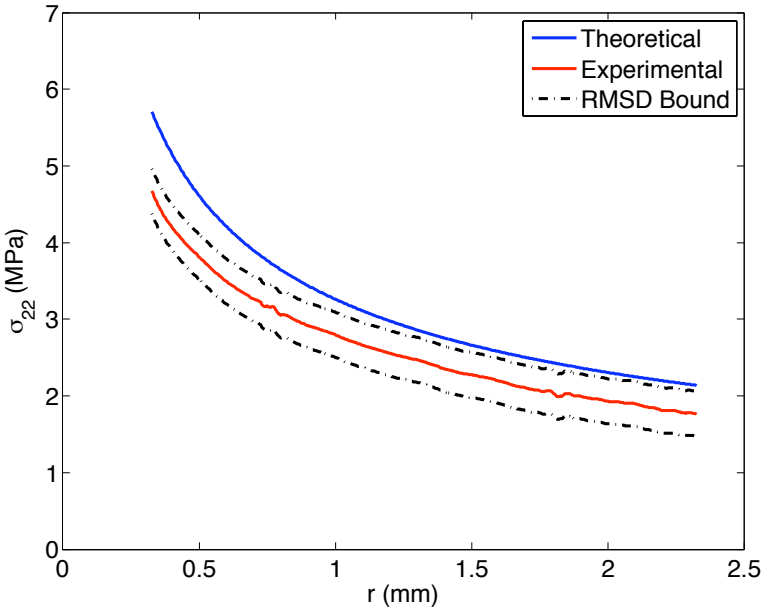

(a) σ_{yy} vs. r for $\theta = 0$

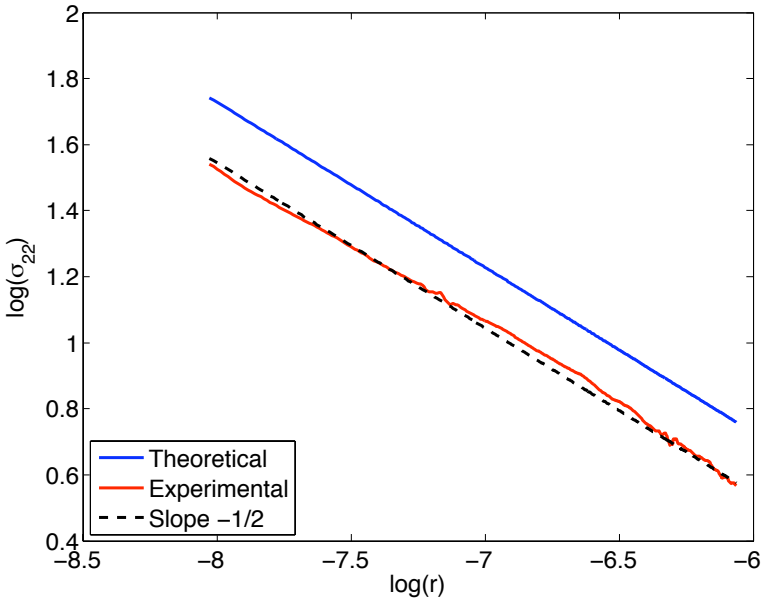

(b) $\log(\sigma_{yy})$ vs. $\log(r)$ for $\theta = 0$

Figure 4.45: Experimental and theoretical data for σ_{yy} along $\theta = 0$ for specimen HomC1 for $K_I = 0.259$ MPa$\sqrt{\text{m}}$ and $K_{II} = 5.0$ kPa$\sqrt{\text{m}}$: The experimental data is slightly lower than the theoretical data, but with similar $r^{-1/2}$ dependence seen by the near $-1/2$ slope on the log-log plot of σ_{yy} versus r.